Original Article

MOLECULAR METABOLISM

High fat diet blunts stress-induced hypophagia and activation of Glp1r dorsal lateral septum neurons in male but not in female mice

Michelle B. Bales [1,a], Samuel W. Centanni [1,2,b], Joseph R. Luchsinger [1,c], Payam Fathi [1], Jessica E. Biddinger [1], Thao D.V. Le [1], Kaitlyn Ginika Nwaba [1], Isabella M. Paldrmic [1], Danny G. Winder [1,2], Julio E. Ayala [1,2,3,*]

ABSTRACT

Objective: While stress typically reduces caloric intake (hypophagia) in chow-fed rodents, presentation of palatable, high calorie substances during stress can increase caloric consumption (i.e. "comfort feeding") and promote obesity. However, little is known about how obesity itself affects feeding behavior in response to stress and the mechanisms that can influence stress-associated feeding in the context of obesity.
Methods: We assessed food intake and other metabolic parameters in lean and obese male and female mice following acute restraint stress. We also measured real-time activity of glucagon-like peptide-1 (Glp1) receptor (Glp1r)-expressing neurons in the dorsal lateral septum (dLS) during stress in lean and obese mice using fiber photometry. Glp1r activation in various brain regions, including the dLS, promotes hypophagia in response to stress. Finally, we used inhibitory Designer Receptors Activated Exclusively by Designer Drugs (DREADDs) to test whether activation of Glp1r-expressing neurons in the LS is required for stress-induced hypophagia.
Results: Lean male mice display the expected hypophagic response following acute restraint stress, but obese male mice are resistant to this acute stress-induced hypophagia. Glp1r-positive neurons in the dLS are robustly activated during acute restraint stress in lean but not in obese male mice. This raises the possibility that activation of dLS Glp1r neurons during restraint stress contributes to subsequent hypophagia. Supporting this, we show that chemogenetic inhibition of LS Glp1r neurons attenuates acute restraint stress hypophagia in male mice. Surprisingly, we show that both lean and obese female mice are resistant to acute restraint stress-induced hypophagia and activation of dLS Glp1r neurons.
Conclusions: These results suggest that dLS Glp1r neurons contribute to the hypophagic response to acute restraint stress in male mice, but not in female mice, and that obesity disrupts this response in male mice. Broadly, these findings show sexually dimorphic mechanisms and feeding behaviors in lean vs. obese mice in response to acute stress.

Keywords Glucagon-like peptide-1; Restraint stress; Lateral septum; Food intake; Fiber photometry; Struggle behavior

1. INTRODUCTION

Stress is a ubiquitous environmental factor that can affect feeding behavior. In rodents, the typical response to stress is reduced caloric intake (hypophagia) and weight loss. However, when presented with palatable, calorie-dense substances, the hypophagic effect of stress is attenuated and, over time, chronic stress can accelerate the progression towards obesity [10,25,38,48]. While research on the relationship between stress and obesity has primarily focused on how stress contributes to the development of obesity, much less is known about how obesity itself affects the response to stress or how mechanisms regulating feeding behavior in response to stress are affected in the obese state. We focus here on identifying mechanisms that influence feeding behavior in the setting of obesity in response to acute stress. This is a necessary first step since adaptive mechanisms in the setting of acute stress may become maladaptive in the setting of chronic stress.

Glucagon-like peptide-1 (Glp1) has emerged as a key molecule that regulates the response to stress. Although it is widely recognized as a gut secreted peptide that stimulates insulin secretion by engaging a pancreatic β-cell Glp1 receptor (Glp1r), Glp1 is also secreted from preproglucagon (PPG) neurons in the nucleus of the tractus solitarius

[1]Department of Molecular Physiology & Biophysics, Vanderbilt University School of Medicine, 2215 Garland Avenue, Nashville, TN 37232, USA [2]Vanderbilt Center for Addiction Research, Vanderbilt University School of Medicine, 2215 Garland Avenue, Nashville, TN 37232, USA [3]Vanderbilt Mouse Metabolic Phenotyping Center, Vanderbilt University School of Medicine, 2215 Garland Avenue, Nashville, TN 37232, USA

[a] Present address: Department of Psychology, Program in Neuroscience, Florida State University, 1107 West Call Street, Tallahassee, FL 32306, USA
[b] Present address: Department of Physiology and Pharmacology, Wake Forest School of Medicine, 475 Vine Stress, Winston-Salem, NC 27101, USA
[c] Present address: Department of Psychiatry, Yale University, 300 George Street, New Haven, CT 06511, USA

*Corresponding author. Department of Molecular Physiology & Biophysics Vanderbilt University School of Medicine 2215 Garland Avenue 742 Robinson Research Building Nashville, TN 37232, USA. E-mail: julio.e.ayala@vanderbilt.edu (J.E. Ayala).

Abbreviations: Glp1, Glucagon-like peptide-1; Glp1r, Glucagon-like peptide-1 receptor; dLS, Dorsal Lateral Septum; PPG, preproglucagon; NTS, Nucleus tractus solitarius

Received February 10, 2022 • Revision received July 19, 2022 • Accepted August 2, 2022 • Available online 8 August 2022

https://doi.org/10.1016/j.molmet.2022.101571

(NTS) [21]. Activation of NTS PPG neurons reduces food intake and body weight in rodents [19,21]. This is likely due, at least in part, to subsequent stimulation of Glp1r signaling in brain regions innervated by NTS PPG neurons, such as the lateral parabrachial nucleus (LpBN) and hypothalamus, since targeting Glp1r agonists to these brain regions also reduces food intake and body weight [1,31]. Reduced food intake (hypophagia) is a typical stress response in rodents, and several lines of evidence suggest that endogenous Glp1 action in the brain plays an important role in this behavior. Central administration of Glp1 induces cFos expression, a marker for neuronal activity, in stress-related corticotropin releasing hormone (CRH)-producing neurons of the paraventricular nucleus (PVN) [27] and stimulates the hypothalamic-pituitary-adrenal (HPA) axis in rats [24]. Acute stress causes activation of PPG neurons in the NTS in rats [28,33,34] and mice [59], and chemogenetic inhibition of NTS PPG neurons attenuates acute stress-induced hypophagia [21]. Additionally, intracerebroventricular (ICV) delivery of the Glp1r antagonist Exendin (9—39) (Ex9) reduces the ability of acute restraint stress to promote hypophagia [34]. Targeting Ex9 to specific brain regions such as the bed nucleus of the stria terminalis (BNST) [65] and the PVN [69] shows that inhibition of the Glp1r in these regions attenuates the hypophagic response to stress.

The lateral septum (LS) is another brain region that may be targeted by Glp1 to regulate feeding behavior in response to stress. The LS is a relay center for various brain regions, and it plays a key role in modulating behavioral responses to anxiety and stress [43,54]. Restraint stress increases cFos expression in the LS in rodents [3,39,47], and direct activation of Glp1r-expressing neurons in the LS reduces food intake [5]. This suggests that LS Glp1 action promotes hypophagia in response to restraint stress. This is further supported by studies showing that inhibition of LS Glp1r signaling, specifically in the dorsal LS (dLS), attenuates restraint stress-induced hypophagia in rodents [58,59]. Interestingly, restraint stress hypophagia is attenuated in rats given intermittent access to sucrose prior to stress, and this is associated with blunted activation of LS neurons compared to chow-fed controls [35,39]. Taken together, these results suggest that LS Glp1r neurons promote restraint stress hypophagia, and the activation of these neurons in response to restraint stress is attenuated by exposure to palatable, high calorie substances.

The present studies assessed the effect of obesity on food intake and dLS Glp1r neuronal activity in response to acute restraint stress in mice and whether dLS Glp1r neurons are necessary for stress-induced hypophagia. Our findings demonstrate that obese male mice are resistant to acute restraint stress-induced hypophagia, and this is associated with decreased activation of dLS Glp1r neurons. Furthermore, inhibition of LS Glp1r neuronal activity blunts acute restraint stress-induced hypophagia in lean male mice, suggesting that LS Glp1r neurons mediate hypophagia following acute restraint stress. Interestingly, we find that both lean and obese female mice are resistant to the hypophagic response following acute restraint stress, and they are also resistant to the activation of dLS Glp1r neurons during restraint.

2. MATERIALS AND METHODS

2.1. Subjects

All mice were housed in the Vanderbilt University Medical Center animal vivarium and kept on a standard 12hr/12hr light/dark cycle. Mice had *ad libitum* access to distilled water and were either maintained on a chow diet (LabDiet, 5L0D) from the time of weaning or were given a high fat diet (HFD, Research Diets Inc., D12492) from six weeks of age. All animals were 4—6 months old at the time of testing. Experimental procedures were approved by The Institutional Animal Care and Use Committee at Vanderbilt University.

2.2. Handling acclimation

To prevent stress from handling alone, mice underwent a handling acclimation procedure modified from [45] for five days prior to testing. On Day 1, the experimenter placed a newly-gloved hand in the cage for 90 s and the animal was allowed to explore the gloved hand. This only occurred on Day 1. The mouse was then placed on top of the hand which gently lifted a few inches from the cage floor for a few seconds and was then placed back down slowly for the mouse to dismount the hand. This movement was repeated 5—10 times depending on the demeanor of the mouse (e.g., if the mouse was slow to move away from the hand, indicating acclimation to the hand, the experimenter would repeat this only 5 times, but if the mouse was quick to dismount the hand, the experimenter would lift the mouse 10 times to acclimate further). On the final hand lift, the mouse was held higher in the air ($\sim$20 cm) for 5 s on Day 1, 10 s on Day 2, and 15 s on Day 3. On the last two days of the handling acclimation procedure, the mouse was simply placed into the hand, stroked a few times, and then weighed.

2.3. Energy balance parameters following restraint stress

Chow- and HFD-fed male and female C57BL/6J mice (#000664, The Jackson Laboratory) were individually housed at least one week before being singly-housed in a Promethion metabolic system (Sable Systems, Inc.). Once in the Promethion, body weights were monitored daily. The handling acclimation procedure (see 2.2) was begun only after mice regained their initial body weight ($\sim$1 week). Following the handling acclimation procedure mice underwent restraint stress for 1 h prior to dark onset. Chow-fed mice were gently guided into a 50 mL conical tube (1 inch diameter) that was modified to have the same number of air holes and tail/nose holes as restrainers for obese mice (at least 1.5 inches in diameter; Plas Labs, #552-BSRR). Control (no restraint stress) mice were picked up by the tail and placed back down in the cage. Food intake, water intake, energy expenditure, substrate oxidation (Respiratory Exchange Ratio (RER)), and locomotor activity were recorded continuously every 5 min overnight. Meal patterns (meal number, intermeal interval, meal size, meal duration) were calculated by the Promethion software. A meal was defined as any removal of food from the hopper that lasted a minimum of 30 s with a maximum removal of 0.5 g and a maximum interval of 300 s between meals. Mice that spilled or cashed $>$0.5 g of food in a 5 min bin were removed from the analysis.

2.4. Glp1r neuronal activity during restraint stress

Real-time activity of dLS Glp1r neurons during restraint stress was measured using fiber photometry. Struggle behavior was assessed during the fiber photometry sessions using DeepLabCut (DLC) video analysis as previously described [32].

2.4.1. Surgery

Chow- and HFD-fed male and female mice expressing Cre recombinase under the control of the *glp1r* locus (Glp1r-ires-Cre; #029283, The Jackson Laboratory) crossed with a tdTomato reporter (Ai14D; #007914, The Jackson Laboratory) were deeply anesthetized and secured into an Angle Two stereotaxic instrument (Leica Biosystems). A craniotomy was performed under isoflurane anesthesia (2—3%). The Cre-dependent intracellular Ca2+ sensor (GCaMP7f) or control GFP (see Table 1) was then infused into the dLS (300 nL in the left

hemisphere; 50 nL/s) using a microinjection syringe pump and a 33G needle (WPI) at a 22.05° angle. The coordinates for the injection were +0.5 mm rostral, +/−0.3 mm lateral, and −3.0 mm ventral. A borosilicate mono fiber-optic cannula (Doric Lenses Inc.) with a 400 μm core diameter was then implanted into the dLS using the same coordinates as the GCaMP7 and was secured to the skull with two small screws (Plastics One) and dental cement. Mice were given three weeks to recover and to allow time for the GCaMP7 to express before testing.

2.4.2. Recording procedure

Mice underwent the handling acclimation protocol (see 2.2). Mice were also acclimated to the fiber-optic patch cord, which attaches to the fiber-optic cannula, two days prior to testing. On the test day, animals acclimated to the testing room for at least 1 h. Each mouse was connected to the fiber-optic patch cord and allowed 5 min of acclimation before recording began. The recordings were captured with an LED-based fiber photometry system (Tucker−Davis Technologies, TDT, Model is RZ5P) with Synapse acquisition and analysis software that uses real-time lock-in amplification and signal demodulation to detect in vivo fluorescence lifetime measurements and photometry recordings through optical fibers. Each recording consisted of a single-mode excitation fiber originating from a 470 nM wavelength LED, and the multimode detection fiber that was surgically implanted and collects bulk fluorescence induced by the GCaMP7. Recordings were made during the restraint period as well as 10 min before and 10 min after the restraint stress with no pause in recording. Mice were also video recorded (Logitech PRO HD Webcam C920) for assessment of struggle behavior (see 2.4.5 below). Restrainers varied in diameter based on the weight of the mouse to help account for variability in level of restraint. Mice between 21 and 30.9 g were gently guided into a clear acrylic restraint device described in [32] with a 1 in. diameter (Vanderbilt Kennedy Center Scientific Instrumentation Core). Mice that were 31−40.9 g went into a restrainer that was at least 1.5 inches in diameter (Plas Labs, #552-BSRR).

2.4.3. Fiber-optic cannula and GCaMP7 confirmation

After testing was complete, animals were deeply anesthetized and transcardially perfused with PBS followed by 4% paraformaldehyde (PFA). Brains were placed in 4% PFA for at least 24 h then transferred to a 20% sucrose in PBS solution to cryoprotect the brains for at least 48 h, all at 4 °C. Brains were carefully blocked and then mounted on a freezing microtome and sectioned coronally at 35 μm. Sections were then mounted on Superfrost slides and coverslipped with ProLong Gold Antifade Mountant in order to histologically confirm the placement of the GCaMP7 and the fiber-optic cannula. Sections were examined under a fluorescent microscope for correct cannula placement and fluorescent signal of GCaMP7. Only animals with correct fiber-optic cannula placement were included in the analysis.

2.4.4. Fiber photometry data analysis

Each recording was broken down into seven segments comprising of 8-minutes of recording, leaving 2 min to account for time it took to get the mouse into the restrainer, and then analyzed separately to account for a natural drift in baseline. Raw photon count was converted to $\Delta F/F_0$ using a segmented normalization procedure with a bin of 4 s and Ca2+ transients was determined using a Savitsky−Golay filter and empirically identified kinetic parameters using the MLspike algorithm in MATLAB. The mLspike algorithm, which is a validated way to impute spike frequency based on Ca2+ transients [15], was used to measure spike frequency. Area under the curve was measured and statistics were calculated in Prism 9 (GraphPad). Group differences were assessed with two-way ANOVAs and Bonferroni's multiple comparisons test. P values of $< .05$ were considered significant.

2.4.5. Head movement analysis

Videos from fiber photometry test day were cropped to include only the time when the animal was in the restrainer. One minute was taken off the beginning and the end of each video to account for some variation in start and stop times across recordings. These 58 min videos were then analyzed for head movements using DLC as described in [32] and briefly described here. Tail movement analysis was omitted due to the restrainers for larger mice obscuring the tails from view. Regardless, head movement accounts for the majority of a struggle behavior [32]. Following hand-scoring of head movements on similarly restrained mice, where bouts were separated by < 0.7 s pause, DLC was used to track the same head movements. DLC allows for automated video scoring by tracking points across time using similar methods for scoring manually [36,42]. The point that was used to track head movements, and was consistent across recordings, was a small piece of green tape attached to the fiber-optic patch cable. DLC was trained to automatically track this point after manually locating the point on at least 495 images. The statistical software R (R Foundation for Statistical Computing, [49]) and the "tidyverse" package [62] was used to make the point (the green tape) an X/Y position based on pixels into a speed of the head movement for each frame of the video (10 fps). Head movements were counted when the frame had a speed greater than one standard deviation above the lower 95% of frame speeds. Normalizing the speed of the head movement in this way allowed for more consistency across animals to account for small differences in restrainer and camera placement, though the experimenter took care to mitigate changes in camera and restrainer placement during testing. AUC and maximum peak amplitude were calculated for the 5 s after bout onset to normalize across bouts. Maximum peak was time-locked to the fiber photometry recording in

Table 1 − Materials used.

Substance	Application	Source
pGP-AAV9-syn-FLEX-jGCaMP7f-WPRE	Fiber photometry	Addgene (Cat. # 104,492)
Clozapine N-oxide (CNO)	Activator of muscarinic DREADDs	Tocris (Cat. #4936)
pAAV8-hSyn-DIO-HA-hM4D (Gi)-IRES-mCitrine	Inhibitory DREADD	Addgene (Plasmid #50455)
DAPI (4′,6-Diamidino-2-Phenylindole, Dihydrochloride)	Nuclear and chromosome counterstain	Invitrogen (Cat. #D1306)
HA-Tag (C29F4) Rabbit mAb	Primary antibody to visualize HA tag for DREADD experiments	Cell Signaling (Cat. #3724)
cFos (9F6) Rabbit mAb #2250	Primary antibody to visualize cFos for DREADD experiments	Cell Signaling (Cat. #2250)
Alexa Fluor® 488 goat anti-rabbit IgG (H + L)	Secondary to visualize HA tag for DREADD experiments	Invitrogen (Cat. #A-1108)
Goat anti-Rabbit IgG (H + L) Highly Cross-Adsorbed Secondary Antibody, Alexa Fluor™ 647	Secondary to visualize cFos for DREADD experiments	Invitrogen (Cat. #A-21245)
SYNAPSE, MATLAB, ImageJ, Graphpad Prism, R, Tidyverse	Analysis software	Vanderbilt University

MATLAB. Head movement figures were created in R with the ggplot2 package [63].

2.4.6. Chemogenetic modulation of dLS Glp1r neurons

In Glp1r-Cre+ male mice crossed with a tdTomato reporter, inhibiting (pAAV8-hSyn-DIO-HA-hM4D (Gi)-IRES-mCitrine; Addgene) designer receptors exclusively activated by designer drugs (DREADD) were delivered into the dLS as described for GCaMP7 (see 2.4.1) except that 300 nL of DREADD AAV was injected into each hemisphere, totaling 600 nL (50 nL/s) via a microinjection syringe pump and a 33G needle (WPI) at a 22.05° angle. Surgery was performed under anesthesia (2–3% isoflurane), and mice were given at least three weeks to recover and to allow time for the DREADD to express before testing with CNO.

Following recovery, mice were individually housed at least one week before going into the Promethion and then acclimated to the Promethion for one week and underwent the handling acclimation procedure (see 2.2). Mice also acclimated to injections with saline (i.p.) four days prior to test days. Treatment groups were balanced based on body weight. Inhibiting DREADD experiments were performed with a crossover design in which mice were restrained with either saline or CNO injections on Test Days 1 and 4 or remained unrestrained with saline or CNO injections on Test Days 2 and 3. Saline and CNO were injected 30 min before restraint stress or no restraint stress which was administered 1 h before dark onset for Test Days 1–3. There were two days between test days during which all mice continued receiving i. p. saline injections. Test Day 4 was followed by transcardial perfusion, so no food intake was measured. Only mice with confirmed DREADD expression in LS were included in the analyses and group differences were assessed with two-way ANOVAs and Bonferroni's multiple comparisons test. $P < 0.05$ were considered significant. Outlier tests were conducted by measuring mean food intake every 2 h during the 12 h dark cycle (6 time points) Mice with food intake values greater than 2x standard deviation from the mean in 3 or more consecutive time points were excluded as outliers.

2.4.7. DREADD confirmation

After food intake testing was complete, animals were given saline or CNO (2 mg/kg, i. p.) and 30 min later were either restrained or left unrestrained for 1 h. Mice were then anesthetized and transcardially perfused with PBS followed by freshly prepared 4% paraformaldehyde (PFA). Brains were then extracted and placed in 4% PFA for at least 24 h then transferred to a cryoprotectant solution of 20% sucrose in PBS for at least 48 h, all at 4 °C. Brains were then coronally sectioned on a freezing microtome at 35 μm.

Sections were selected at 25, 50, and 75% the length of dLS, at approximately 1.0, 0.5, and 0.0 mm AP based on anatomical landmarks [18] for free-floating immunohistochemistry. To stain for the HA tag to visualize the DREADD expression, sections first permeabilized in 0.4% Triton X-100 in PBS for 1 h at room temperature. Sections then sat in blocking buffer (1% Bovine Serum Albumin, 5% Normal Goat Serum [NGS] in the same Triton X-100 solution) for an hour at room temperature before sitting in the primary HA tag rabbit antibody (Table 1; 1:500) in blocking buffer for 48 h at 4 °C. Following rinses (3 × 10 min) in the Triton X-100 solution, sections were kept in a goat anti-rabbit Alexa Fluor 488 secondary (Table 1; 1:250) in blocking buffer solution for 2 h at room temperature. Rinses (3 × 10 min) in the Triton X-100 solution occurred before applying a DAPI (1:25,000) in PBS solution (15 min). One more rinse, this time in PBS (10 min), was administered before sections were mounted onto glass slides and allowed to dry overnight. Slides were then coverslipped with ProLong Gold Antifade Mountant. Slides were imaged on the LSM710 confocal at 40x or 5x to confirm DREADD expression.

A similar protocol was used on free-floating sections to stain for cFos. Sections adjacent to those chosen for HA tag immunohistochemistry were selected. First, sections sat in a blocking buffer (2% NGS, 0.1% Triton X-100 in PBS) for 1 h at room temperature. Primary rabbit antibody for cFos (Table 1; 1:1000) was added to blocking buffer and sections stayed in the solution at 4 °C for 48 h. Sections were then rinsed in PBS (4 × 10 min) and then placed in a goat anti-rabbit Alexa Fluor 647 secondary (Table 1; 1:500) in blocking buffer solution for 1 h at room temperature. Another round of rinses in PBS (4 × 10 min) was administered before sections sat in a DAPI solution (1:25,000 in PBS; 15 min) followed by one rinse in PBS (10 min). Sections were then mounted onto glass slides, dried overnight, and coverslipped with ProLong Gold Antifade Mountant. Slides were imaged on a LSM710 confocal at 5x to assess cFos expression. cFos quantification was performed using Fiji [52] by three independent experimenters blind to the conditions. Values represent averages of counts from the three experimenters.

3. RESULTS

3.1. Energy balance parameters in lean and obese mice following restraint stress

After twelve weeks on HFD male mice were obese compared to chow-fed males (t-test with Bonferroni correction: $P < 0.0001$; Figure 1A). Female mice were also obese following HFD feeding compared to female chow-fed mice (t-test with Bonferroni correction: $P < 0.0001$; Figure 1A). As expected, food intake decreased following restraint stress in lean male mice shown by a main effect of the 1 h restraint on chow intake over the 12 h following dark onset (Two-way ANOVA: Interaction, $F(144, 2736) = 5.898$, $P < 0.0001$; Stress Effect, $F(1, 19) = 4.528$, $P = 0.0367$; Figure 1B). Consistent with previous studies [65], decreased food intake was not evident until ~4 h post restraint stress. Contrasting the phenotype in lean mice, there was no effect of the 1 h restraint on food intake in obese male mice over the same 12 h following dark onset (Two-way ANOVA: Interaction, $F(144, 2736) = 0.3109$, $P > 0.9999$; Stress Effect, $F(1, 19) = 0.02640$, $P = 0.8727$; Figure 1C). When cumulative food intake data are plotted in 2 h intervals, there is a significant interaction between diet and stress with time (Two-way ANOVA: Interaction, $F(15, 190) = 6.198$, $P < 0.0001$) with a significant main effect of diet and stress (Two-way ANOVA: $F(3, 38) = 4.337$, $P = 0.0101$; Figure 1D). Tukey's posthoc test showed that cumulative food intake was significantly different between chow-fed and HFD-fed mice that had undergone restraint at 8, 10, and 12 h post-restraint ($P = 0.0052$, 0.0017, and 0.0013, respectively; Figure 1D). Meal pattern analysis showed a significant interaction of diet and stress over time for meal number (Two-way ANOVA: Interaction, $F(15, 190) = 1.887$, $P = 0.0266$; Figure 1E) with Tukey's posthoc test revealing a significant decrease in meal number 6–8 h post dark onset in chow-fed restrained mice compared to chow-fed controls ($P = 0.0326$). There was no significant effect of stress on meal number in HFD-fed mice, but meal number was significantly higher in restrained HFD-fed mice compared to restrained chow-fed mice at 6–8 h and 8–10 h post dark onset ($P = 0.001$ and 0.0088, respectively). There was a significant interaction of diet and stress condition over time for intermeal intervals (Two-way ANOVA: Interaction, $F(15, 190) = 1.765$, $P = 0.0423$; Figure 1F), but there was no main effect of stress on intermeal interval in either chow- or HFD-fed mice. There was no significant interaction between diet and stress over time on meal duration (Two-way ANOVA: Interaction, F (15,

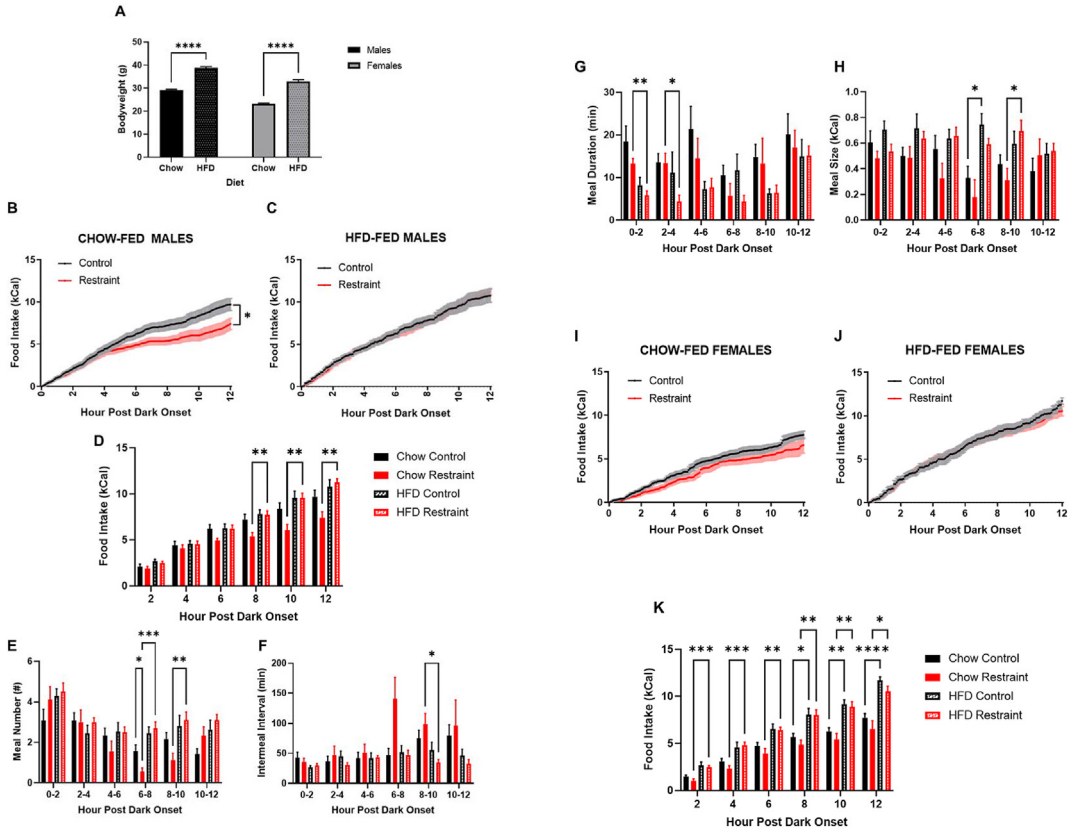

Figure 1: Restraint Stress Hypophagia in Lean Male Mice but Not in Obese Male or Lean or Obese Female Mice. A) Body weight of chow-fed and HFD-fed male and female mice on the day of restraint. B-D; I–K) Food intake following no restraint (Control; black lines/bars) or restraint stress (Restraint; red lines/bars) which occurred for 1 h prior to dark onset in lean male (B–D) and female (I–K) wild-type mice. E-H) Meal patterns (meal number, intermeal interval, meal duration, and meal size) in lean (solid bars) and obese (hatched bars) male mice. *P < 0.05, **P < 0.01, ***P < 0.001, ****P < 0.0001 in a t-test (A) or Two-way ANOVA (B–K). Data are presented as Mean ± SEM. N = 9–12/group.

190) = 0.7188, P = 0.7637; Figure 1G) and size (Two-way ANOVA: Interaction, F (15, 190) = 0.1354, P = 0.1742; Figure 1H). Tukey's posthoc analysis showed meal duration was shorter in HFD-fed restrained compared to chow-fed restrained mice at 0–2 h and 2–4 h post dark onset (P = 0.0011 and 0.0205, respectively). Meal size was also larger in HFD-fed restrained compared to chow-fed restrained mice at 8–10 h post dark onset (P = 0.0313).

There was no interaction of diet and stress over time in female mice that were fed a chow diet (Two-way ANOVA: Interaction, F (144, 2016) = 0.9579, P = 0.6236; Stress Effect, F (1, 14) = 2.621, P = 0.1278; Figure 1I) or female mice fed a HFD (Two-way ANOVA: Interaction, F (144, 2016) = 0.5848, P > 0.9999; Stress Effect, F (1, 14) = 0.05391, P = 0.8198; Figure 1J). When food intake in chow- and HFD-fed female mice is plotted every 2 h there is an interaction between diet and stress over time (Two-way ANOVA: Interaction, F (15, 140) = 4.980, P < 0.0001; Figure 1K), but Tukey's post-hoc test shows no significant effect of stress on food intake in chow-fed or HFD-fed female mice. Significant differences are only observed across diets within treatment conditions (control or stress). Taken together, these results show that HFD-fed male mice are resistant to acute restraint stress-induced hypophagia, but female mice do not display acute restraint stress-induced hypophagia regardless of metabolic status.

Gas exchange measurements (i.e., rate of oxygen consumed (VO_2) and rate of carbon dioxide produced (VCO_2)) were continuously taken in the Promethion to estimate the rate of calories burned, or energy expenditure (EE), as well as an index of substrate oxidation, or the Respiratory Exchange Ratio (RER). There was a significant interaction between stress and time on EE in chow-fed (Two-way ANOVA: Interaction, F (159, 3021) = 5.057, P < 0.0001; Figure 2A) and HFD-fed (Two-way ANOVA: Interaction: F (159, 3021) = 3.123, P < 0.0001; Figure 2B) male mice, although there was no main effect of stress in either chow-fed (Stress Effect: F (1, 19) = 1.324, P = 0.2642) or HFD-fed (Stress Effect: F (1, 19) = 2.072, P = 0.1663) mice during the time spanning both the stress episode and the 12 h post-stress. Since EE increased during the restraint period (Figure 2A,B, yellow box), we analyzed the effect of stress on EE only during the 1 h restraint period. There was a significant interaction between diet and stress over time (Two-way ANOVA: Interaction, F (42, 532) = 1.545, P < 0.0001) including an increase in EE for both chow-fed (Tukey's multiple comparisons test, P < 0.0001) and HFD-fed control mice (Tukey's multiple comparisons test, P < 0.0001) but not between chow- and HFD-fed stressed mice (Tukey's multiple comparisons test, P = 0.5592; Figure 2C). Elevated EE during restraint could be due to increased breathing and muscle contractions as the mice struggle within the restrainer. The observation that EE is increased during restraint stress in both lean and obese male mice suggests that both lean and obese mice experience stress equally, and the absence of stress-induced hypophagia in obese mice is not due to a difference in the stress experience. A more direct measure of stress (i.e., struggle behavior) will be discussed below.

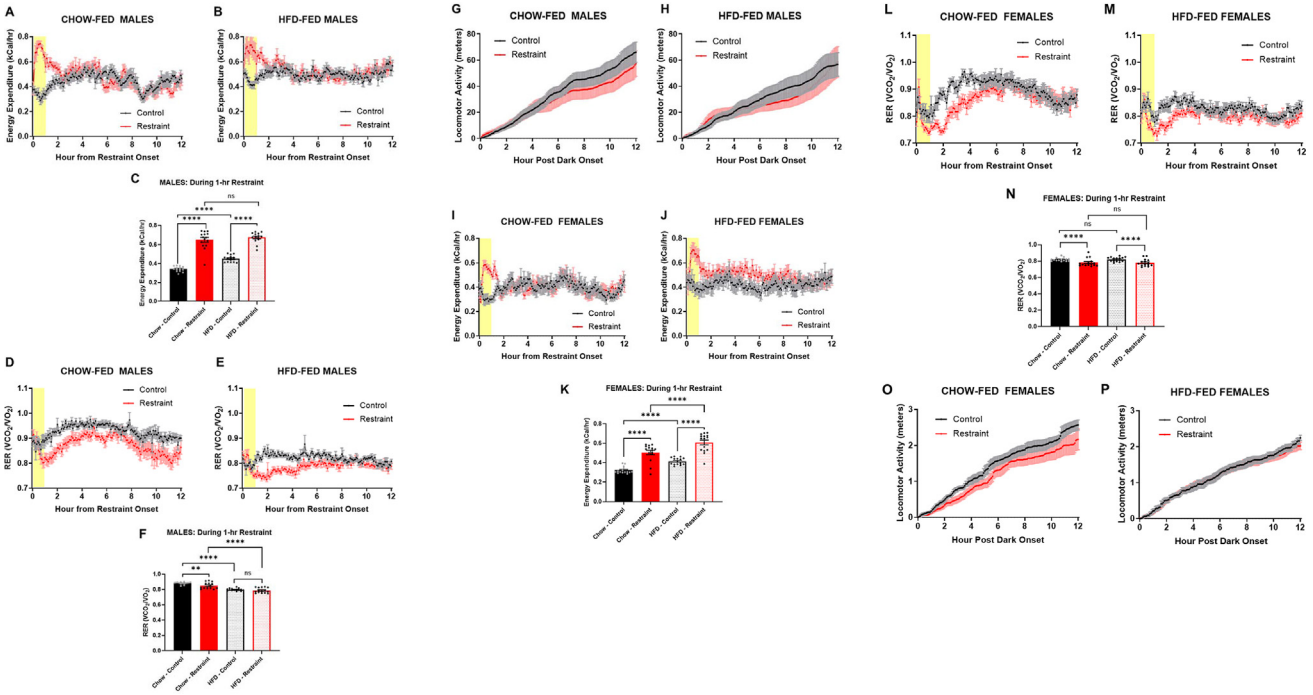

Figure 2: Metabolic Readings Following Restraint Stress or No Restraint Stress in Lean and Obese Male and Female Mice. EE in chow-fed (A) and HFD-fed (B) control (black line/bar) and restrained (red line/bar) male mice during 1 h control or restraint stress period (yellow highlight) and the subsequent 12 h. C) Average EE during the control and restraint period. RER in chow-fed (D) and HFD-fed (E) control (black line/bar) and restrained (red line/bar) male mice during 1 h control or restraint stress period (yellow highlight) and the subsequent 12 h. F) Average RER during the control and restraint period. Locomotor activity in chow-fed (G) or HFD-fed (H) male mice following no restraint (Control; black) or restraint stress (Restraint; red) 1 h prior to dark onset. EE in chow-fed (I) and HFD-fed (J) control (black line/bar) and restrained (red line/bar) female mice during 1 h control or restraint stress period (yellow highlight) and the subsequent 12 h. K) Average EE during the control and restraint period. RER in chow-fed (L) and HFD-fed (M) control (black line/bar) and restrained (red line/bar) female during 1 h control or restraint stress period (yellow highlight) and the subsequent 12 h. N) Average RER during the control and restraint period. Locomotor activity in chow-fed (O) or HFD-fed (P) female mice following no restraint (Control; black) or restraint stress (Restraint; red) 1 h prior to dark onset. $^{**}P < 0.01$, $^{****}P < 0.0001$ in a Two-way ANOVA. Data are presented as Mean ± SEM. N = 8–12/group.

RER is indicative of substrate oxidation, with a RER of 1.0 indicating pure carbohydrate oxidation and a RER of 0.7 indicating pure fat oxidation. In chow-fed male mice, there was a significant interaction between stress and time (Two-way ANOVA: Interaction, F (159, 3021) = 1.542, $P < 0.0001$; Figure 2D) with a main effect of stress to lower RER (Stress Effect: F (1, 19) = 10.86, P = 0.003). There was also a significant interaction of stress and time in HFD-fed male mice (Two-way ANOVA: Interaction, F (159, 3021) = 3.527, $P < 0.0001$; Figure 2E) with a main effect of stress to also lower RER (Stress Effect: F (1,19) = 22.78, P = 0.0001). Focusing on RER during the 1 h stress episode, there was a significant interaction between diet and stress over time (Two-way ANOVA: F (42, 532) = 3.660, $P < 0.0001$), with a significant decrease in RER during stress in chow-fed mice (Tukey's multiple comparisons test, $P < 0.0001$; Figure 2F) but not in HFD-fed mice (Tukey's multiple comparisons test, P = 0.3688; Figure 2F). This reduced RER is indicative of increased reliance on fat oxidation. Although there was a significant interaction between time and stress on locomotor activity in chow-fed male mice (Two-way ANOVA: Interaction, F (144, 2736) = 1.307, P = 0.0096; Figure 2G), there was no main effect of stress (F (1, 19) = 0.4568, P = 0.5073). There was also no interaction between time and stress or a stress effect on locomotor activity in HFD-fed male mice (Two-way ANOVA: Interaction, F (144, 2736) = 0.8658, P = 0.8708; Stress Effect, F (1, 19) = 0.1624, P = 0.6915; Figure 2H).

For female mice, there was a significant interaction between stress and time on EE in chow-fed (Two-way ANOVA: Interaction, F (159, 2226) = 3.276, $P < 0.0001$; Figure 2I) and HFD-fed (Two-way ANOVA: Interaction, F (159, 2226) = 3.198, $P < 0.0001$; Figure 2J) but no overall main effect of stress (Chow-fed Stress Effect: F (1, 4) = 0.06664, P = 0.8001; HFD-fed Stress Effect: F (1, 14) = 1.666, P = 0.2177) during the time spanning both the stress episode and the 12 h post-stress. As with male mice, we analyzed the effect of stress on EE during only the 1 h stress period. There was a significant interaction between stress and time on EE during the 1 h restraint period (Two-way ANOVA: F (42, 532) = 2.152, $P < 0.0001$) with an increase in EE in both chow-fed (Tukey's multiple comparisons test, $P < 0.0001$) and HFD-fed (Tukey's multiple comparisons test, $P < 0.0001$) female mice (Figure 2K).

Regarding RER, there was a significant interaction between conditions over time for chow-fed (Two-way ANOVA: Interaction, F (159, 2226) = 2.712, $P < 0.0001$; Figure 2L) and HFD-fed (Two-way ANOVA: Interaction, F (159, 2226) = 1.563, $P < 0.0001$; Figure 2M) female mice. There was a tendency for a main effect of stress on RER in chow-fed female mice (Stress Effect: F (1, 14) = 4.054, P = 0.0637) and a significant main effect of stress in HFD-fed female mice (Stress Effect: F (1, 14) = 10.21, P = 0.0065). Assessing the effect of stress on RER only during the 1 h restraint period shows a significant interaction between stress and time (Two-way ANOVA: F

(45, 520) = 2.503, P < 0.0001; Figure 2N) with stress promoting lower RER in both chow-fed (Tukey's multiple comparisons test, P < 0.0001) and HFD-fed (Tukey's multiple comparisons test, P < 0.0001) female mice. This reduced RER is indicative of increased reliance on fat oxidation.

Locomotor activity was not affected by acute restraint stress in either chow-fed (Two-way ANOVA: Interaction, F (159, 2206) = 0.9579, P = 0.6236; Stress Effect, F (1, 14) = 2.621, P = 0.1278; Figure 2O) or HFD-fed (Two-way ANOVA: Interaction, F (159, 2226) = 0.5848, P > 0.9999; Stress Effect, F (1, 14) = 0.05391, P = 0.8198; Figure 2P) female mice.

3.2. Activity of dLS Glp1r neurons in lean and obese mice during restraint stress

We used fiber photometry to assess real-time activity of dLS Glp1r-expressing neurons during acute restraint stress in lean and obese mice. Figure 3A is a representative image showing targeted expression of the genetically-encoded GCaMP calcium sensor in the dLS of Glp1r-Cre; tdTomato mice and correct probe targeting. Restraint stress rapidly stimulated the activity of Glp1r-expressing dLS neurons as shown by significantly increased peak area and spike frequency normalized to the pre-restraint stress period. This effect is easily observed in representative dLS Glp1r neuronal traces of one lean male (Figure 3B,C) and one obese male mouse (Figure 3D,E) during non-restraint and then during restraint the following day. Overall, obese male mice had a lower normalized spike frequency and normalized GCaMP calcium peak area (spikes only) from the GCaMP7 signal compared to lean male mice (Figure 3F,G). Two-way ANOVA revealed a diet effect for both normalized spike frequencies (Interaction: F (1, 12) = 5.439, P = 0.038) and normalized peak areas (Interaction: F (1, 12) = 5.849, P = 0.0324; and Bonferroni's multiple comparisons test revealed significant differences at segment two and three, P = 0.0364 and P = 0.011, respectively) in male mice. Contrasting this, stress stimulated dLS Glp1r neuronal activity in female mice, but the diet effect for normalized peak areas (Interaction: F (1, 20) = 0.661, P = 0.426; Time Effect: F (2.844, 56.88) = 6.435, P = 0.0010; Diet Effect: F (1, 20) = 0.6614, P = 0.4256) and spike frequencies (Interaction: F (1, 20) = 0.134, P = 0.718; Time Effect: F (2.007, 38.13) = 3.505, P = 0.0399; Diet Effect: F (1, 19) = 1.227, P = 0.2818) was not significantly different between lean and obese female mice (Figure 3H,I).

3.3. Head movement analysis

One factor that could explain reduced activation of Glp1r-expressing dLS neurons in obese mice during stress is that restraint may not be as physically stressful to obese mice as it is to lean mice. During restraint stress, rodents engage in periodic struggle behavior characterized by head and/or tail movement. This struggle behavior is believed to be representative of active escape behavior and is associated with increased neuronal activity in stress-related brain regions such as the BNST [32]. We used a custom restraint stress apparatus that enabled analysis of head movement during the fiber photometry experiments and used this as an index of the degree of stress experienced by lean and obese mice. There was no difference in average length of struggle bouts (Bartlett test for homogeneity = 0.03701; therefore, we ran a non-parametric test, Kruska–Wallis test, chi-squared = 6.4693, df = 3, P = 0.09088; Figure 4A), number of head movement bouts (Bartlett test = 0.0575; Kruska–Wallis test, chi-squared = 5.7777, df = 3; P = 0.1229; Figure 4B), or total struggle time in a bout (Bartlett test = 0.004091; Kruska–Wallis test, chi-squared = 2.5923, df = 3; P = 0.4588; Figure 4C), between lean and obese mice. Taken together, the absence of any differences in struggle behavior between lean and obese male or female mice suggests that lean and obese mice experience restraint stress similarly.

Measuring head movement during the fiber photometry experiments allowed for direct comparison of time-locked active struggling to calcium transients measured in Glp1r-expressing dLS neurons (Figure 4D,E). In this analysis, time = 0 represents the onset of the struggle bout, and GCaMP activity is shown for the 5 s before and after the onset of the struggle bout. Comparing head movements time-locked with fiber photometry recording across maximum peaks show that calcium transient amplitude increases prior to the struggle onset in both lean and obese male mice, but lean males display a continued rise in calcium transient amplitude following struggle onset whereas calcium transient amplitude flattened after struggle onset in obese male mice. This results in a greater maximum peak amplitude in lean vs. obese males after the initiation of the struggle bout (paired t-tests with Bonferroni correction, p = 0.007; Figure 4D). Calcium transient amplitudes continued to rise following struggle onset in female mice but began to flatten 1–2 s after struggle onset. There was no difference in maximum peaks between lean and obese females (p = 1.0; Figure 4E). Analysis of area under the curve (AUC) shows greater AUC in lean vs. obese males (paired t-tests and Bonferroni correction p = 0.003; Figure 4F), but no difference between lean and obese females (p = 1.0; Figure 4F). Taken together, these data suggest that lean and obese males experience restraint stress equally (i.e., there is no difference in struggle behavior), but the response of dLS Glp1r neurons is increased in lean, male mice. Furthermore, there are no apparent differences between lean and obese female mice. Since dLS Glp1r signaling contributes to acute restraint stress-induced hypophagia in mice [59], these results also align with our observation that stress-induced hypophagia is blunted by obesity in male mice.

3.4. Effect of inhibiting dLS Glp1r neurons on stress-induced hypophagia

To determine whether activation of LS Glp1r neurons is necessary for acute stress-induced hypophagia, we combined restraint stress with chemogenetic inhibition of LS Glp1r neurons using a G_i-coupled DREADD in Glp1r-Cre; tdTomato mice. Restraint stress promoted hypophagia in saline-treated mice (Two-way ANOVA: Interaction, F (144, 3168) = 4.280, P < 0.0001; Stress Effect, F (1, 22) = 15.81, P = 0.0006; Figure 5A). Inhibiting LS Glp1r neurons completely blocked stress-induced-hypophagia (Two-way ANOVA: Interaction, F (144, 3600) = 0.3018, P > 0.9999; Stress Effect, F (1, 25) = 309.8, P = 0.6388; Figure 5B). Representative images of cFos in Control + Saline (Figure 5C), Restraint + Saline (Figure 5D), Control + CNO (Figure 5F), and Restraint + CNO (Figure 5G) show increased cFos in the dLS in response to restraint stress with saline treatment, but this is reduced with CNO treatment. Verification of DREADD expression primarily to the dLS is shown by immunostaining of the HA tag expressed by the virally delivered construct (Figure 5E,H). Representative images also show tdTomato$^+$ (i.e., Glp1r$^+$) cells, cFos, and co-localization of cFos with tdTomato$^+$ cells in the dLS (Figures 5I-5Q). Restraint stress increased cFos compared to the control condition, and this effect of restraint on cFos was reduced following CNO injection. A representative image shows co-localization of HA (i.e., DREADD expression) and tdTomato$^+$ cells with sparse cFos in the dLS in a restrained mouse following CNO injection (Figure 5R). ~90% of cFos$^+$ cells in the dLS under any condition were also tdTomato$^+$. Counts of cFos$^+$/tdTomato$^+$ cells in the dLS were quantified (Figure 5S). There was no significant difference in cFos between saline and CNO-treated

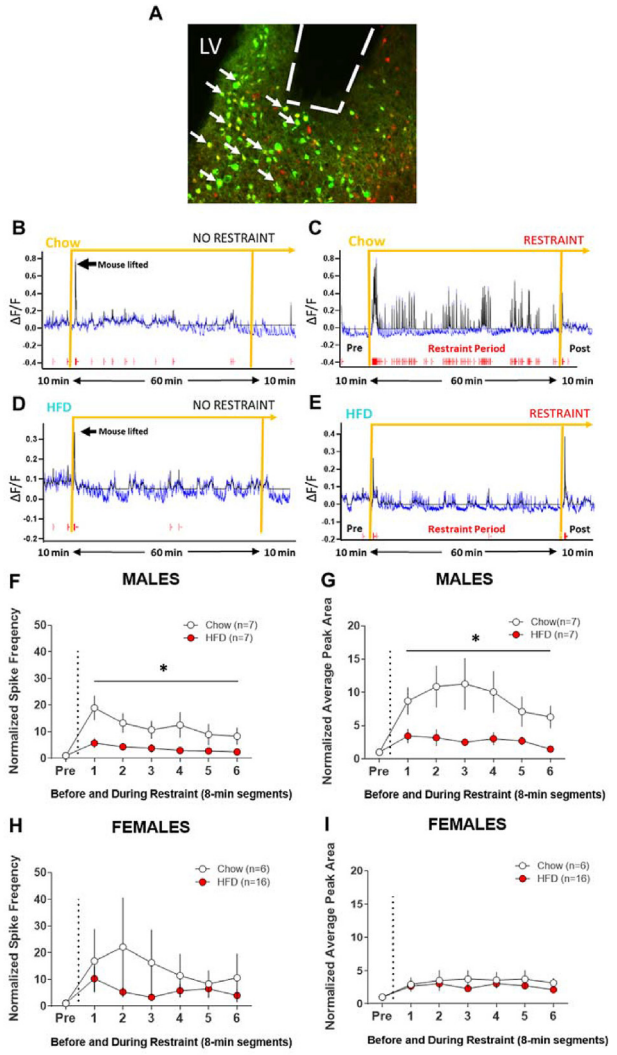

Figure 3: Restraint Stress Increases dLS Glp1r Neuronal Activity in Lean Male Mice but Not in Obese Male or Lean or Obese Female Mice. A) Representative fluorescent image of unamplified GCaMP expression (green), native tdTomato in Glp1r^{+} neurons (red), and co-localization (yellow, highlighted with white arrows) in the dLS. Of 159 red cells (Glp1r^{+}) counted, 146 were yellow, yielding an efficiency of GCaMP expression in Glp1r^{+} neurons of 91.82%. Of 162 green cells (GCaMP^{+}), 16 were not yellow (Glp1r^{-}), yielding non-selective expression of 9.88%. Hashed lines outline the fiber-optic cannula placement. LV = lateral ventricle. Scale bar = 200 μm. Fluorescent signal, a proxy for neuronal activity, in a lean (B, C) and an obese (D, E) male mouse during no restraint (B, D) and restraint (C, E). Orange line and initial spike in fluorescent signal occurred when mouse was lifted by the tail to simulate putting the mouse in a restrainer (No Restraint [B, D]) or to put the mouse in a restrainer (Restraint C, E). The mLspike algorithm, which is a validated way to impute spike frequency based on Ca2+ transients, was used to measure spike (red hatch marks) frequency in MATLAB and generated the 'best trajectory' of calcium values (black lines) [15]. Fiber photometry recordings of Glp1r neurons in the dLS in male (F, G) and female (H, I) Glp1r-Cre mice. Recordings adjusted for baseline fluctuations and segmented into six bins to assess average frequency per minute of calcium spikes (F, H) and area under the peaks (G, I), in arbitrary units, normalized to pre-restraint. #P $<$ 0.05 in a Two-way ANOVA; *P $<$ 0.05 in a t-test. Data are presented as Mean ± SEM. N = 6–16/group.

control (no restraint) mice (Two-way ANOVA with Tukey's multiple comparisons, P = 0.8809). Restraint stress significantly increased cFos in the dLS in saline-treated mice (Two-way ANOVA with Tukey's multiple comparisons, P = 0.0002). There was no significant difference in cFos between control and restrained CNO-injected mice (P = 0.2313), and restrained mice injected with CNO had reduced cFos expression compared to saline-injected restrained mice (P = 0.0158). These results strongly suggest that activation of LS Glp1r^{+} neurons is required for acute restraint stress-induced hypophagia.

4. DISCUSSION

Although stress can promote weight gain and obesity, little is known about the effects of stress in the context of already established obesity. Clinical studies suggest that obese individuals are more susceptible to the negative effects of stress, such as depression, which can lead to a deleterious feed-forward cycle of "comfort feeding" [9,11,14,26,44,55,61]. This provides an opportunity to identify mechanisms that regulate caloric intake in response to stress and how these mechanisms may be altered in the setting of obesity. We used a combination of sophisticated metabolic phenotyping and real-time neuronal activity measurements to show for the first time that Glp1r-expressing neurons in the dLS are rapidly and robustly activated during acute restraint stress in lean male mice, and this is markedly attenuated in obese male mice. Our subsequent observation that chemogenetic inhibition of LS Glp1r neurons attenuates acute restraint stress-induced hypophagia suggests that impaired activation of these neurons in obesity contributes to increased caloric intake in response to stress. This identifies a novel target that can explain deleterious changes in feeding behavior at the intersection of stress and obesity. Our results are in line with previous studies showing that inhibition of Glp1r signaling in the dLS attenuates restraint hypophagia in rodents [58,59]. This suggests that acute restraint stress-induced hypophagia requires stimulation of Glp1r signaling and the activity of Glp1r-expressing neurons. One possibility is that stimulation of Glp1r signaling enhances the activity of dLS Glp1r-expressing neurons as has been previously shown in Glp1r-expressing neurons in the paraventricular hypothalamus [30]. The LS is innervated by Glp1-producing NTS PPG neurons [50,65], so if obesity impairs Glp1 production or another function of NTS PPG neurons, this could lead to attenuated activation of dLS Glp1r neurons. Interestingly studies show that expression of Glp1-producing PPG mRNA in the NTS is actually increased in obese rats [8,60]. This raises the possibility that obesity is associated with central Glp1 resistance, as has been previously suggested in rats [41,64]. If Glp1r signaling in the dLS is necessary for stimulation of dLS Glp1r neuronal activity, then a resistance to Glp1 could contribute to the reduced activation of dLS Glp1r neurons during stress we observe in obese male mice.

Previous studies on the effect of obesogenic diets on stress and feeding behavior have primarily provided substances such as sucrose or HFD either shortly before or concomitant with the onset of stress. Short-term access to these substances generally impairs stress-induced hypophagia [10,13,35,38,40,48]. Novelty, palatability, and rewarding aspects of sucrose and fat are likely to be key contributors to increased intake even in the face of stress. It is not clear whether and to what degree these characteristics are still relevant following chronic exposure to HFD in the present studies. Thus, we cannot conclude that obesity itself rather than exposure to the HFD is what impaired stress-induced hypophagia in the present studies. Future experiments will test whether short-term exposure to HFD impairs stress-induced hypophagia in mice presented with either HFD or chow after restraint stress. Furthermore, it will be of interest to determine the

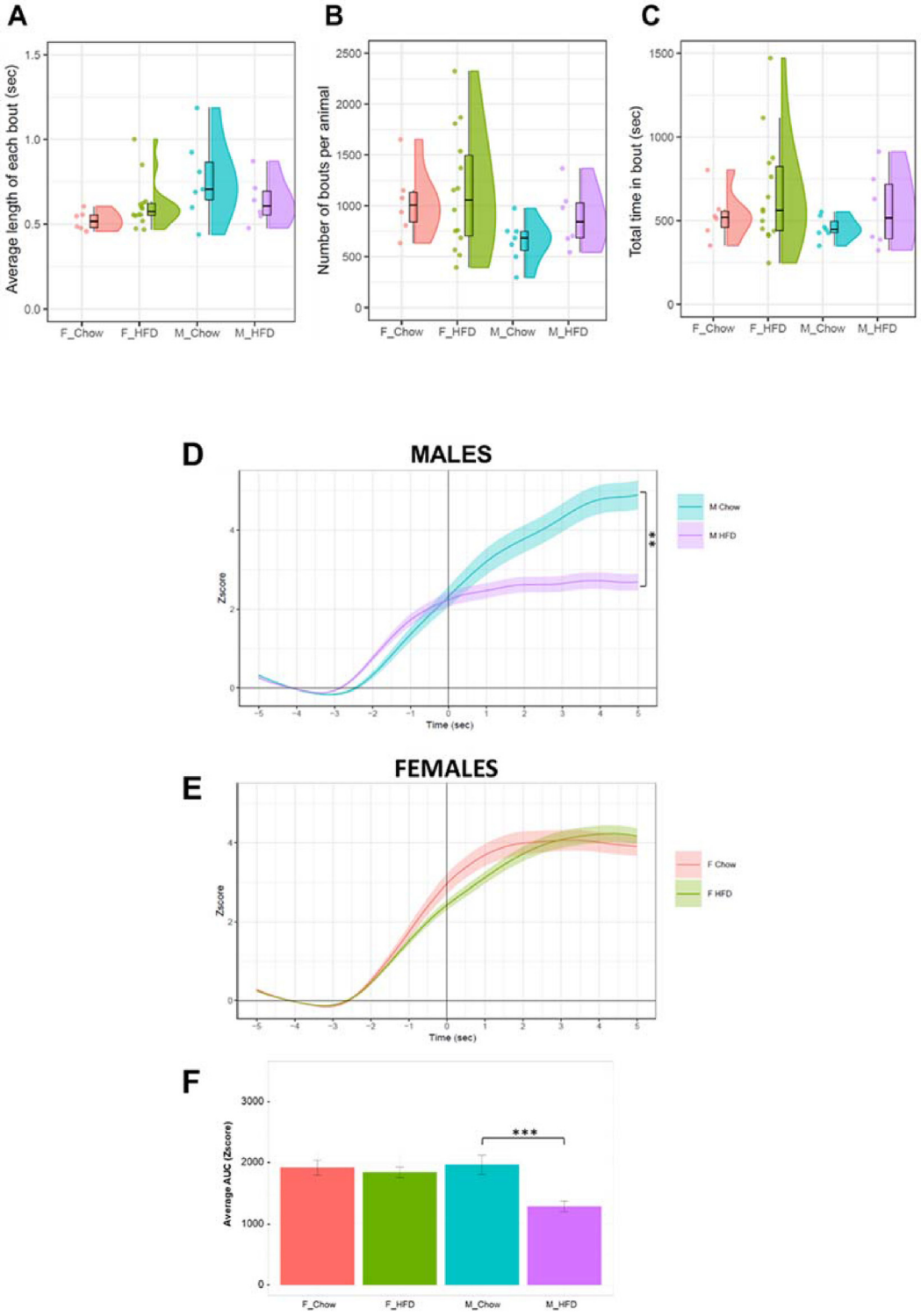

Figure 4: Struggle Behaviors Show Lean and Obese mice Struggled Similarly and dLS Glp1r Neurons are Activated during Struggle in Lean Male Mice compared to Obese Male Mice, whereas Neuronal Responses in Lean and Obese Female Mice do Not Differ during Struggle. Struggle analysis showed no significant differences between dietary conditions within sex suggesting that chow-fed and HFD-fed mice experienced the restraint stress similarly. Average length of each bout (A), number of bouts per animals (B), and total time in bout (C) were analyzed. Male (D) and female (E) fiber photometry recordings time-locked to the struggle analysis. Maximum peaks were calculated for the 5s after bout onset to normalize across bouts and time-locked to the fiber photometry recordings via MATLAB. Movement bout begins at zero seconds. Shaded area is SEM. (F) Average AUC by group. $^{**}P < 0.01$; $^{***}P < 0.001$. ($N = 6–14$/group).

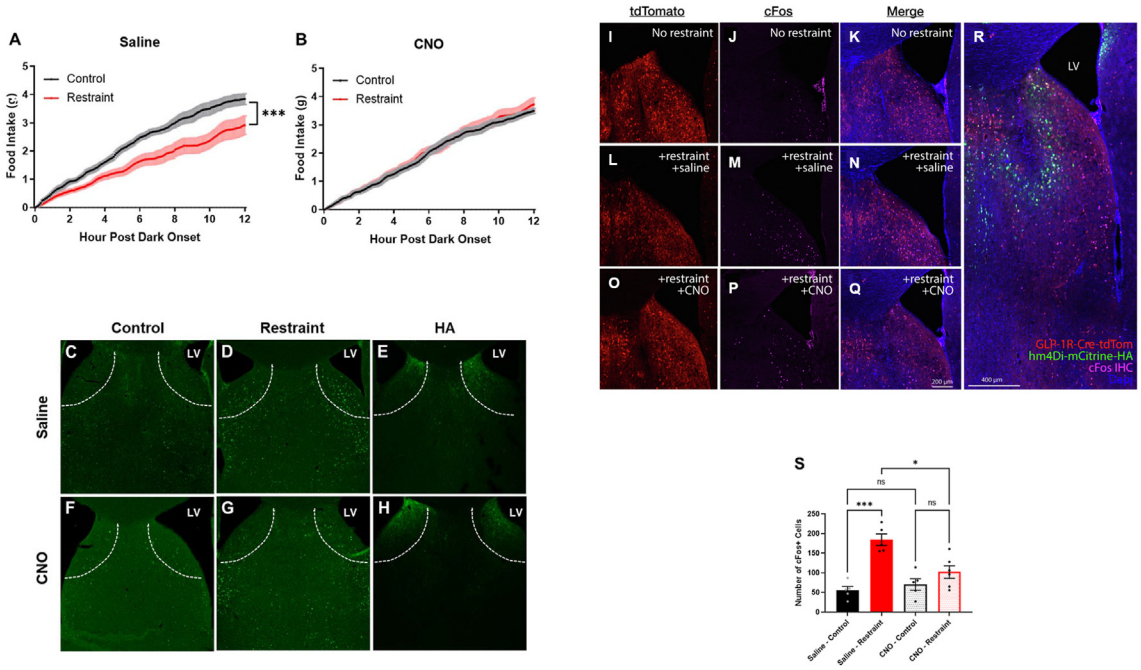

Figure 5: Inhibiting dLS Glp1r Neurons Blunts Stress-Induced Hypophagia. Food intake in male Glp1r-Cre; tdTomato mice expressing inhibitory DREADD in the dLS following saline (A) or CNO injection (B; 2 mg/kg, i. p.) 30 min before either restraint or no restraint 1 h before dark onset. ***P $<$ 0.0001 in a Two-way ANOVA. Data are presented as Mean $\pm$ SEM. N $=$ 12–13/group. C–H) Fluorescent images of dLS, outlined in hatched lines, in saline-injected (C–E) and CNO-injected (F–H) mice showing cFos in control (C, F) and restraint stressed (D, G) mice and HA tag confirming inhibitory DREADD expression (E, H). I-R) Higher magnification representative fluorescent images of dLS showing native tdTomato fluorescence (red), cFos (cyan), and merge (magenta) in saline-treated control (I–K), saline-treated restraint stressed (L–N), and CNO-treated restraint stressed (O–Q) Glp1r-Cre; tdTomato mice as well as cFos, native tdTomato fluorescence, and HA tag (i.e., DREADD; green) in a restraint stressed, CNO-treated mouse (R). S) cFos quantification of control and restrained mice given either saline or CNO (2 mg/kg, i. p.) 90 min before perfusion. *P $<$ 0.05, ***P $<$ 0.001. Data are presented as Mean $\pm$ SEM. N $=$ 5–6/group. LV $=$ lateral ventricle.

effect of short-term exposure to HFD on stress-induced LS Glp1r neuronal activity. Restraint stress induced activation of LS neurons is attenuated in rats that had been previously provided intermittent access to sucrose [35,38], raising the possibility that short-term exposure to palatable substances specifically mitigates the response of LS Glp1r-expressing neurons to stress. Although mice were acclimated to individual housing for one week prior to being housed in the metabolic chambers and were maintained in those chambers for an additional week prior to testing, we cannot exclude the possibility that isolation stress affects the activity of dLS Glp1r neurons and feeding behavior. Our observation that chemogenetic inhibition of LS Glp1r neurons attenuates acute restraint stress-induced hypophagia suggests that activation of these neurons is necessary for the hypophagic effect of stress. This is supported by a recent observation that chemogenetic activation of Glp1r expressing neurons in the lateral septum mimics the effect of stress and reduces food intake [5]. This leads us to propose that stress activates dLS Glp1r neurons, consequently resulting in hypophagia, but in the setting of obesity, the impaired activation of dLS Glp1r neurons directly contributes to the attenuation of acute stress-induced hypophagia. This assigns a key role for dLS Glp1r neurons in the regulation of caloric intake following stress.

Obesity elevates basal corticosterone levels in rodents, and stress subsequently increases corticosterone levels equally in lean and obese mice [4,6,22,53,57]. This suggests that lean and obese rodents experience stress equally. However, since we used larger restrainers to accommodate obese mice for our stress tests, a possible explanation for the blunted stress-induced hypophagia and dLS Glp1r neuronal activation in obese mice is that obese mice were simply not as stressed in the larger restrainers. We used two types of noninvasive measurements to assess the degree of stress experienced by all groups. Performing experiments in metabolic cages demonstrated that EE increases during the restraint stress bout. We interpret this increase in EE as resulting from struggling behavior (e.g., increased muscle contractions and breathing) while in the restrainer. The observation that EE increased equally in both lean and obese mice during restraint suggests that lean and obese mice equally struggle during this procedure. This was verified by our innovative video-based DLC analysis showing that there was no difference in struggle behavior between lean and obese mice. The ability to time-lock GCaMP7 signals to struggle behavior revealed an interesting response. For each struggle bout, dLS Glp1r neuronal activity increased equally between lean and obese mice beginning 2–3 s prior to struggle onset. Whereas dLS Glp1r neuronal activity continued to rise in lean mice after the onset of struggle, this neuronal activity plateaued upon struggle onset in obese mice. This suggests that activity of dLS Glp1r neurons is coupled to struggle behavior, and obesity interferes with this coupling.

One of our novel findings is that female mice are resistant to the hypophagic effects of acute restraint stress regardless of whether they are lean or obese. Sex can affect various responses to stress in rodents [20,23,29,37,56], including effects on feeding behavior [46,67]. The directionality of the effect and whether there is even a sex-dependent response to stress depends on the type, duration, and/or intensity of the stressor as well as other factors such as age of the mice and time of day in which the stressor is executed [17]. In agreement with our findings, a recent study used novelty-suppressed feeding (NSF) to show

that latency to consume food was equally increased in male and female mice, but while novel environment stress reduced food intake in male mice, it had no effect on food intake in female mice [17]. Furthermore, when rendered obese, both male and female mice displayed hyperphagia in response to novel environment stress [17]. Interestingly, another study showed the opposite effect, with female, but not male, mice displaying reduced food intake during a novelty-suppressed feeding test [66]. These discrepant findings are likely due to differences in which the NSF protocols were conducted [17,66]. Nevertheless, our observation that there was no difference in dLS Glp1r neuronal activity during stress between lean and obese female mice further supports the proposed role for dLS Glp1r neurons in the regulation of post-stress feeding. We cannot exclude the possibility that stress can affect feeding behavior and/or dLS Glp1r neuronal activity during specific phases of the estrous cycle. Egan and colleagues showed that a limited sucrose intake paradigm reduces the hypothalamic-pituitary-adrenal (HPA) axis response to stress during proestrus/estrus but not during diestrus 1/diestrus 2 [16]. Including more female mice in the fiber photometry experiments and measuring estrous cycles or recording only on specific days of the cycle would help determine any differences in dLS Glp1r responses across the cycle and between dietary conditions. From an evolutionary perspective, one advantage of females maintaining normal food intake under stressful conditions could be to prepare for or to sustain a pregnancy. The LS also has other sexually dimorphic functions. Only female juvenile mice with vasopressin administered into the LS reduce social play behaviors, and male juveniles with vasopressin injected into the LS increase anxiety-like behaviors [12]; see [7] for review of other sex differences in mechanisms of anxiety).

Taken together, our results combine novel approaches to show that stress activates dLS Glp1r neuronal activity in lean male mice, but obesity is associated with impaired activation of dLS Glp1r neurons during stress and, as a consequence, attenuated hypophagia. In response to chronic stress, this could provide a mechanism for increased susceptibility to stress in obese individuals and further exacerbate weight gain. Future studies will focus on downstream targets of the LS that regulate feeding behavior. The LS extends projections to brain regions involved in the regulation of food intake, such as the lateral hypothalamus. Interestingly, LS Glp1r neurons are GABAergic [51,68], suggesting that stress-induced activation of LS Glp1r neurons exerts inhibitory control on post-synaptic targets. Although we focus on obesity in these studies, it is clear that obesogenic substances also impair both the hypophagic response to stress and activation of LS neurons in the absence of obesity [35,38]. Future studies will also determine whether exposure to obesogenic substances in the absence of obesity specifically attenuates stress-induced activation of LS Glp1r neurons and whether this contributes to impaired hypophagia following stress.

FUNDING

This work was supported by the National Institutes of Health (5T32 DK007563, 5R37 AA019455, 4R00 AA027774, and 5U2C DK059637).

CONFLICT OF INTEREST

None

DATA AVAILABILITY

Data will be made available on request.

ACKNOWLEDGEMENTS

The Vanderbilt Mouse Metabolic Phenotyping Center (MMPC; National Institutes of Health 5U2C DK059637), especially Louise Lantier, PhD and Merrygay James, helped run all experiments that used the Promethion (Sable Systems International). We also had assistance with the fiber photometry experiments from Gregory Salimando, PhD (baseline analysis), Andrew Gaulden, Amanda Morgan, PhD (AUC fiber photometry analysis), and Kellie Williford (restraint device design). Microscopy was performed in part through the use of the Vanderbilt Cell Imaging Shared Resource ([CISR] supported by NIH grants CA68485, DK20593, DK58404, DK59637 and EY08126) and Jenny Schafer, PhD (CISR Managing Director) was very helpful in obtaining images.

REFERENCES

[1] Alhadeff, A.L., Baird, J.P., Swick, J.C., Hayes, M.R., Grill, H.J., 2014. Glucagon-like peptide-1 receptor signaling in the lateral parabrachial nucleus contributes to the control of food intake and motivation to feed. Neuropsychopharmacology 39(9):2233–2243. https://doi.org/10.1038/npp.2014.74.

[3] Anthony, T.E., Dee, N., Bernard, A., Lerchner, W., Heintz, N., Anderson, D.J., 2014. Control of stress-induced persistent anxiety by an extra-amygdala septohypothalamic circuit. Cell 156(3):522–536. https://doi.org/10.1016/j.cell.2013.12.040.

[4] Appiakannan, H.S., Rasimowicz, M.L., Harrison, C.B., Weber, E.T., 2020. Differential effects of high-fat diet on glucose tolerance, food intake, and glucocorticoid regulation in male C57BL/6J and BALB/cJ mice. Physiology & Behavior 215:112773. https://doi.org/10.1016/j.physbeh.2019.112773.

[5] Azevedo, E.P., Tan, B., Pomeranz, L.E., Ivan, V., Fetcho, R., Schneeberger, M., et al., 2020. A limbic circuit selectively links active escape to food suppression. Elife 9. https://doi.org/10.7554/eLife.58894.

[6] Balsevich, G., Uribe, A., Wagner, K.v., Hartmann, J., Santarelli, S., Labermaier, C., et al., 2014. Interplay between diet-induced obesity and chronic stress in mice: potential role of FKBP51. Journal of Endocrinology 222(1):15–26. https://doi.org/10.1530/JOE-14-0129.

[7] Bangasser, D.A., Cuarenta, A., 2021. Sex differences in anxiety and depression: circuits and mechanisms. Nature Reviews Neuroscience. https://doi.org/10.1038/s41583-021-00513-0.

[8] Barrera, J.G., Jones, K.R., Herman, J.P., D'Alessio, D.A., Woods, S.C., Seeley, R.J., 2011. Hyperphagia and increased fat accumulation in two models of chronic CNS glucagon-like peptide-1 loss of function. Journal of Neuroscience 31(10):3904–3913. https://doi.org/10.1523/JNEUROSCI.2212-10.2011.

[9] Barrington, W.E., Beresford, S.A.A., McGregor, B.A., White, E., 2014. Perceived stress and eating behaviors by sex, obesity status, and stress vulnerability: findings from the vitamins and lifestyle (VITAL) study. Journal of the Academy of Nutrition and Dietetics 114(11):1791–1799. https://doi.org/10.1016/j.jand.2014.03.015.

[10] Bartolomucci, A., Cabassi, A., Govoni, P., Ceresini, G., Cero, C., Berra, D., et al., 2009. Metabolic consequences and vulnerability to diet-induced obesity in male mice under chronic social stress. PLoS One 4(1):e4331. https://doi.org/10.1371/journal.pone.0004331.

[11] Boggiano, M.M., Wenger, L.E., Turan, B., Tatum, M.M., Morgan, P.R., Sylvester, M.D., 2015. Eating tasty food to cope. Longitudinal association with BMI. Appetite 87:365–370. https://doi.org/10.1016/j.appet.2015.01.008.

[12] Bredewold, R., Smith, C.J.W., Dumais, K.M., Veenema, A.H., 2014. Sex-specific modulation of juvenile social play behavior by vasopressin and oxytocin depends on social context. Frontiers in Behavioral Neuroscience 8(JUNE):1–11. https://doi.org/10.3389/fnbeh.2014.00216.

[13] Chuang, J.-C., Perello, M., Sakata, I., Osborne-Lawrence, S., Savitt, J.M., Lutter, M., et al., 2011. Ghrelin mediates stress-induced food-reward behavior

in mice. Journal of Clinical Investigation 121(7):2684–2692. https://doi.org/10.1172/JCI57660.
[14] Coulthard, H., Sharps, M., Cunliffe, L., van den Tol, A., 2021. Eating in the lockdown during the Covid 19 pandemic; self-reported changes in eating behaviour, and associations with BMI, eating style, coping and health anxiety. Appetite 161:105082. https://doi.org/10.1016/j.appet.2020.105082.
[15] Deneux, T., Kaszas, A., Szalay, G., Katona, G., Lakner, T., Grinvald, A., et al., 2016. Accurate spike estimation from noisy calcium signals for ultrafast three-dimensional imaging of large neuronal populations in vivo. Nature Communications 7. https://doi.org/10.1038/ncomms12190.
[16] Egan, A.E., Thompson, A.M.K., Buesing, D., Fourman, S.M., Packard, A.E.B., Terefe, T., et al., 2018. Palatable food affects HPA Axis responsivity and forebrain neurocircuitry in an estrous cycle-specific manner in female rats. Neuroscience 384:224–240. https://doi.org/10.1016/j.neuroscience.2018.05.030.
[17] Francois, M., Canal Delgado, I., Shargorodsky, N., Leu, C.S., Zeltser, L., 2022. Assessing the effects of stress on feeding behaviors in laboratory mice. Elife 11:1–20. https://doi.org/10.7554/eLife.70271.
[18] Franklin, K., Paxinos, G., 2008. The mouse brain atlas in stereotaxic coordinates. In: The spinal cord: a christopher and dana reeve foundation text and atlas. https://doi.org/10.1016/B978-0-12-374247-6.50004-3.
[19] Gaykema, R.P., Newmyer, B.A., Ottolini, M., Raje, V., Warthen, D.M., Lambeth, P.S., et al., 2017. Activation of murine pre-proglucagon-producing neurons reduces food intake and body weight. Journal of Clinical Investigation 127(3):1031–1045. https://doi.org/10.1172/JCI81335.
[20] Hodes, G.E., Pfau, M.L., Purushothaman, I., Francisca Ahn, H., Golden, S.A., Christoffel, D.J., et al., 2015. Sex differences in nucleus accumbens transcriptome profiles associated with susceptibility versus resilience to subchronic variable stress. Journal of Neuroscience 35(50):16362–16376. https://doi.org/10.1523/JNEUROSCI.1392-15.2015.
[21] Holt, M.K., Richards, J.E., Cook, D.R., Brierley, D.I., Williams, D.L., Reimann, F., et al., 2019. Preproglucagon neurons in the nucleus of the solitary tract are the main source of brain GLP-1, mediate stress-induced hypophagia, and limit unusually large intakes of food. Diabetes 68(1):21–33. https://doi.org/10.2337/db18-0729.
[22] Kalyani, M., Hasselfeld, K., Janik, J.M., Callahan, P., Shi, H., 2016. Effects of high-fat diet on stress response in male and female wildtype and prolactin knockout mice. PLoS One 11(11):e0166416. https://doi.org/10.1371/journal.pone.0166416.
[23] Karamihalev, S., Brivio, E., Flachskamm, C., Stoffel, R., Schmidt, M.V., Chen, A., 2020. Social dominance mediates behavioral adaptation to chronic stress in a sex-specific manner. Elife 9:1–18. https://doi.org/10.7554/eLife.58723.
[24] Kinzig, K.P., D'Alessio, D.A., Herman, J.P., Sakai, R.R., Vahl, T.P., Figueredo, H.F., et al., 2003. CNS glucagon-like peptide-1 receptors mediate endocrine and anxiety responses to interoceptive and psychogenic stressors. Journal of Neuroscience 23(15):6163–6170. https://doi.org/10.1523/jneurosci.23-15-06163.2003.
[25] Kinzig, K.P., Hargrave, S.L., Honors, M.A., 2008. Binge-type eating attenuates corticosterone and hypophagic responses to restraint stress. Physiology & behavior 95(1–2):108–113. https://doi.org/10.1016/j.physbeh.2008.04.026.
[26] Laitinen, J., Ek, E., Sovio, U., 2002. Stress-related eating and drinking behavior and body mass index and predictors of this behavior. Preventive Medicine 34(1):29–39. https://doi.org/10.1006/pmed.2001.0948.
[27] Larsen, P.J., Tang-Christensen, M., Jessop, D.S., 1997. Central administration of glucagon-like peptide-1 activates hypothalamic neuroendocrine neurons in the rat*. https://academic.oup.com/endo/article/138/10/4445/2988189.
[28] Leon, R.M., Borner, T., Stein, L.M., Urrutia, N.A., de Jonghe, B.C., Schmidt, H.D., et al., 2021. Activation of PPG neurons following acute stressors differentially involves hindbrain serotonin in male rats. Neuropharmacology 187(February): 108477. https://doi.org/10.1016/j.neuropharm.2021.108477.
[29] Li, K., Nakajima, M., Ibañez-Tallon, I., Heintz, N., 2016. A cortical circuit for sexually dimorphic oxytocin-dependent anxiety behaviors. Cell 167(1):60–72. https://doi.org/10.1016/j.cell.2016.08.067 e11.
[30] Liu, J., Conde, K., Zhang, P., Lilascharoen, V., Xu, Z., Lim, B.K., et al., 2017. Enhanced AMPA receptor trafficking mediates the anorexigenic effect of endogenous glucagon-like peptide-1 in the paraventricular hypothalamus. Neuron 96(4):897–909. https://doi.org/10.1016/j.neuron.2017.09.042 e5.
[31] López-Ferreras, L., Richard, J.E., Noble, E.E., Eerola, K., Anderberg, R.H., Olandersson, K., et al., 2018. Lateral hypothalamic GLP-1 receptors are critical for the control of food reinforcement, ingestive behavior and body weight. Molecular Psychiatry 23(5):1157–1168. https://doi.org/10.1038/mp.2017.187.
[32] Luchsinger, J.R., Fetterly, T.L., Williford, K.M., Salimando, G.J., Doyle, M.A., Maldonado, J., et al., 2021. Delineation of an insula-BNST circuit engaged by struggling behavior that regulates avoidance in mice. Nature Communications 12(1):1–18. https://doi.org/10.1038/s41467-021-23674-z.
[33] Maniscalco, J.W., Rinaman, L., 2017. Interoceptive modulation of neuroendocrine, emotional, and hypophagic responses to stress. Physiology and Behavior 176:195–206. https://doi.org/10.1016/j.physbeh.2017.01.027.
[34] Maniscalco, J.W., Zheng, H., Gordon, P.J., Rinaman, L., 2015. Negative energy balance blocks neural and behavioral responses to acute stress by "silencing" central glucagon-like peptide 1 signaling in rats. Journal of Neuroscience 35(30):10701–10714. https://doi.org/10.1523/JNEUROSCI.3464-14.2015.
[35] Martin, J., Timofeeva, E., 2010. Intermittent access to sucrose increases sucrose-licking activity and attenuates restraint stress-induced activation of the lateral septum. The Australian Journal of Pharmacy: Regulatory, Integrative and Comparative Physiology 298(5):R1383–R1398. https://doi.org/10.1152/ajpregu.00371.2009.
[36] Mathis, A., Mamidanna, P., Cury, K.M., Abe, T., Murthy, V.N., Mathis, M.W., et al., 2018. DeepLabCut: markerless pose estimation of user-defined body parts with deep learning. Nature Neuroscience 21(9):1281–1289. https://doi.org/10.1038/s41593-018-0209-y.
[37] Mcdowell, A.L., Fransen, K.M.H., Elliott, K.S., Elghouche, A., Kostylev, P.V., Dea, P.K.O., et al., 2015. Sex differences and the Impact of chronic stress and recovery on instrumental Learning, 19–21. https://doi.org/10.1155/2015/697659.
[38] Michel, C., Levin, B.E., Dunn-Meynell, A., 2003. Stress facilitates body weight gain in genetically predisposed rats on medium-fat diet. American Journal of Physiology - Regulatory, Integrative and Comparative Physiology 285(4): R791–R799. https://doi.org/10.1152/ajpregu.00072.2003.
[39] Mitra, A., Lenglos, C., Timofeeva, E., 2015. Inhibition in the lateral septum increases sucrose intake and decreases anorectic effects of stress. European Journal of Neuroscience 41(4):420–433. https://doi.org/10.1111/ejn.12798.
[40] Moles, A., Bartolomucci, A., Garbugino, L., Conti, R., Capriolo, A., Coccurello, R., et al., 2006. Psychosocial stress affects energy balance in mice: modulation by social status. Psychoneuroendocrinology 31(5):623–633. https://doi.org/10.1016/j.psyneuen.2006.01.004.
[41] Mul, J.D., Begg, D.P., Barrera, J.G., Li, B., Matter, E.K., D'Alessio, D.A., et al., 2013. High-fat diet changes the temporal profile of GLP-1 receptor-mediated hypophagia in rats. American Journal of Physiology - Regulatory, Integrative and Comparative Physiology 305(1):R68–R77. https://doi.org/10.1152/ajpregu.00588.2012.
[42] Nath, T., Mathis, A., Chen, A.C., Patel, A., Bethge, M., Mathis, M.W., 2019. Using DeepLabCut for 3D markerless pose estimation across species and behaviors. Nature Protocols 14(7):2152–2176. https://doi.org/10.1038/s41596-019-0176-0.
[43] Olds, J., Milner, P., 1954. Positive reinforcement produced by electrical stimulation of septal area and other regions of rat brain. Journal of

Comparative & Physiological Psychology 47(6):419–427. https://doi.org/10.1037/h0058775.

[44] Oliver, G., Wardle, J., 1999. Perceived effects of stress on food choice. Physiology and Behavior 66(3):511–515. https://doi.org/10.1016/S0031-9384(98)00322-9.

[45] Olsen, C.M., Winder, D.G., 2010. Operant sensation seeking in the mouse. Journal of Visualized Experiments 45:4–7. https://doi.org/10.3791/2292.

[46] Pankevich, D.E., Bale, T.L., 2008. Stress and sex influences on food-seeking behaviors. Obesity 16:1539–1544. https://doi.org/10.1038/oby.2008.221.

[47] Patel, S., Roelke, C.T., Rademacher, D.J., Hillard, C.J., 2005. Inhibition of restraint stress-induced neural and behavioural activation by endogenous cannabinoid signalling. European Journal of Neuroscience 21(4):1057–1069. https://doi.org/10.1111/j.1460-9568.2005.03916.x.

[48] Pecoraro, N., Reyes, F., Gomez, F., Bhargava, A., Dallman, M.F., 2004. Chronic stress promotes palatable feeding, which reduces signs of stress: feedforward and feedback effects of chronic stress. Endocrinology 145(8):3754–3762. https://doi.org/10.1210/en.2004-0305.

[49] R Core Team, 2019. R: a language and environment for statistical computing. R Foundation for Statistical Computing.

[50] Rinaman, L., 2010. Ascending projections from the caudal visceral nucleus of the solitary tract to brain regions involved in food intake and energy expenditure. Brain Research 1350:18–34. https://doi.org/10.1016/j.brainres.2010.03.059.

[51] Risold, P.Y., Swanson, L.W., 1997. Chemoarchitecture of the rat lateral septal nucleus. Brain Research Reviews 24(2–3):91–113. https://doi.org/10.1016/S0165-0173(97)00008-8.

[52] Schindelin, J., Arganda-Carreras, I., Frise, E., Kaynig, V., Longair, M., Pietzsch, T., et al., 2012. Fiji: an open-source platform for biological-image analysis. Nature Methods 9:676–682. https://doi.org/10.1038/nmeth.2019.

[53] Sharma, S., Fulton, S., 2005. Diet-induced obesity promotes depressive-like behaviour that is associated with neural adaptations in brain reward circuitry. International Journal of Obesity 37(3):382–389. https://doi.org/10.1038/ijo.2012.48.

[54] Singewald, G.M., Rjabokon, A., Singewald, N., Ebner, K., 2011. The modulatory role of the lateral septum on neuroendocrine and behavioral stress responses. Neuropsychopharmacology 36(4):793–804. https://doi.org/10.1038/npp.2010.213.

[55] Slochower, J., Kaplan, S.P., Mann, L., 1981. The effects of life stress and weight on mood and eating. Appetite 2(2):115–125. https://doi.org/10.1016/S0195-6663(81)80005-0.

[56] Takahashi, A., 2021. Toward understanding the sex differences in the biological mechanism of social stress in mouse models. https://doi.org/10.3389/fpsyt.2021.644161.

[57] Tannenbaum, B.M., Brindley, D.N., Tannenbaum, G.S., Dallman, M.F., McArthur, M.D., Meaney, M.J., 1997. High-fat feeding alters both basal and stress-induced hypothalamic- pituitary-adrenal activity in the rat. American Journal of Physiology - Endocrinology and Metabolism 273(6 36–6):1168–1177. https://doi.org/10.1152/ajpendo.1997.273.6.e1168.

[58] Terrill, S.J., Wall, K.D., Medina, N.D., Maske, C.B., Williams, D.L., 2017. Lateral septum growth hormone secretagogue receptor affects food intake and motivation for sucrose reinforcement. American Journal of Physiology - Regulatory, Integrative and Comparative Physiology 34. https://doi.org/10.1152/ajpregu.00339.2017 ajpregu.00339.

[59] Terrill, S.J., Holt, M.K., Maske, C.B., Abrams, N., Reimann, F., Trapp, S., et al., 2019. Endogenous GLP-1 in lateral septum promotes satiety and suppresses motivation for food in mice. Physiology and Behavior 206(January):191–199. https://doi.org/10.1016/j.physbeh.2019.04.008.

[60] Vrang, N., Larsen, P.J., Jensen, P.B., Lykkegaard, K., Artmann, A., Larsen, L.K., et al., 2007. Upregulation of the brainstem preproglucagon system in the obese Zucker rat. https://doi.org/10.1016/j.brainres.2007.10.026.

[61] Weinstein, S.E., Shide, D.J., Rolls, B.J., Weinstein-Dance, S.E., 1997. Changes in food intake in response to stress in men and women: psychological factors. Appetite 28(1):7–18. https://doi.org/10.1006/appe.1996.0056.

[62] Wickham, H., Averick, M., Bryan, J., Chang, W., McGowan, L., François, R., et al., 2019. Welcome to the tidyverse. Journal of Open Source Software 4(43):1686. https://doi.org/10.21105/joss.01686.

[63] Wickham, H., 2016. ggplot2: elegant graphics for data analysis. Springer.

[64] Williams, D.L., Hyvarinen, N., Lilly, N., Kay, K., Dossat, A., Parise, E., et al., 2011. Maintenance on a high-fat diet impairs the anorexic response to glucagon-like-peptide-1 receptor activation. Physiology & behavior 103(5):557–564. https://doi.org/10.1016/j.physbeh.2011.04.005.

[65] Williams, D.L., Lilly, N.A., Edwards, I.J., Yao, P., Richards, J.E., Trapp, S., 2018. GLP-1 action in the mouse bed nucleus of the stria terminalis. Neuropharmacology 131:83–95. https://doi.org/10.1016/j.neuropharm.2017.12.007.

[66] Yamada, C., Iizuka, S., Nahata, M., Hattori, T., 2020. Vulnerability to psychological stress-induced anorexia in female mice depends on blockade of ghrelin signal in nucleus tractus solitarius. p. 4666–82. https://doi.org/10.1111/bph.15219. July.

[67] Yamada, C., Sadakane, C., Nahata, M., Saegusa, Y., Nakagawa, K., Okubo, N., et al., 2015. Serotonin 2C receptor contributes to gender differences in stress-induced hypophagia in aged mice. Psychoneuroendocrinology 55:81–93. https://doi.org/10.1016/j.psyneuen.2015.02.006.

[68] Zhao, C., Eisinger, B., Gammie, S.C., 2013. Characterization of GABAergic neurons in the mouse lateral septum: a double fluorescence in situ hybridization and immunohistochemical study using tyramide signal amplification. PLoS One 8(8):1–24. https://doi.org/10.1371/journal.pone.0073750.

[69] Zheng, H., Reiner, D.J., Hayes, M.R., Rinaman, L., 2019. Chronic suppression of glucagon-like peptide-1 receptor (GLP1R) mRNA translation in the rat bed nucleus of the stria terminalis reduces anxiety-like behavior and stress-induced hypophagia, but prolongs stress-induced elevation of plasma corticosterone. Journal of Neuroscience 39(14):2649–2663. https://doi.org/10.1523/jneurosci.2180-18.2019.

